A Transconductance-Mode Multifunction Filter with High Input and High Output Impedance Nodes Using Voltage Differencing Current Conveyors (VDCCs)

Montree SIRIPRUCHYANUN[1], *Winai JAIKLA*[2]

[1]Department of Teacher Training in Electrical Engineering, Faculty of Technical Education, King Mongkut's University of Technology North Bangkok, 1518 Pracharat 1 Road, Wongsawang, Bangsue, 10800 Bangkok, Thailand
[2]Department of Engineering Education, Faculty of Industrial Education and Technology, King Mongkut's Institute of Technology Ladkrabang, 1 Chalong Krung 1 Alley, Lat Krabang, 10520 Bangkok, Thailand

montree.s@fte.kmutnb.ac.th, winai.ja@kmitl.ac.th

DOI: 10.15598/aeee.v18i4.3938

Abstract. *The design of transconductance-mode multifunction biquad filter containing three input voltage nodes and single-output current node is proposed. Its circuit principle is emphasized on employing Voltage Differencing Current Conveyor (VDCC) to be an active building block. The proposed filter description uses three VDCCs co-working with two grounded capacitors and three grounded resistors. The synthesis of the proposed multifunction filter is based on avoidance of using multiple-output active elements to achieve commercially available integrated circuits for practical implementation. Additionally, without multiple-output active element, it can alleviate current tracking error from the current mirrors used in output ports. It also decreases the amounts of the transistors inside the active elements. The proposed multifunction filter offers all 5 filter functions, which are non-inverting Low-Pass (LP), non-inverting High-Pass (HP), non-inverting Band-Pass (BP), non-inverting Band-Reject (BR) and also non-inverting All-Pass (AP) functions from same circuit topology under different circuit condition for input signals. Furthermore, the natural frequency for all filtering responses is independently achieved from the bandwidth or the quality factor of the proposed filter. For cascade-able connectivity, the output current port indeed provides a high impedance. In addition, the magnitude of the output current for all filtering functions can be resistively adjusted. The consideration for non-ideal case of the presented multifunction filter is also analyzed. The simulation and experimental results of the presented transconductance multifunction biquad filter based on VDCC practically implemented by the commercially available ICs, LM13700 and AD844 can validate the theoretical anticipation.*

Keywords

Analog circuit, commercially available IC, electronic control, multifunction filter, transconductance-mode, VDCC.

1. Introduction

Analog active filters are essential parts for analog signal processing systems, they are widely employed in many applications, such as communications, audio systems, instrumentation and measurement system, control systems, mobile telecommunication systems [1]. Most of analog filters are designed in second-order system, because second-order (or biquad) filter can be obtained completely by five filtering transfer function forms: Low-Pass (LP), High-Pass (HP), Band-Pass (BP), Band-Reject (BR) and All-Pass (AP). The second-order multifunction filter offers many filtering transfer function forms in the same configuration without modifying circuit scheme. It has obtained significant encouragement and became an interesting research topic. Among several types of the multifunction filters, the Multiple-Input Single-Output (MISO) multifunction filter is an attractive circuit and has been designed over the years [2]. Additionally, Current-Mode

(CM) multifunction filters whose desired parameters are electronically adjusted by relative currents provide several benefits, for example, low power consumption, greater linearity, larger input dynamic range, wider bandwidth, or smaller number of components compared to circuits in voltage-mode configuration using in voltage-mode active devices such as conventional operational amplifiers [3], [4] and [5].

The design and implementation of modern analog signal processing circuits can be categorized into two forms, which are Very Large-Scale Integration (VLSI) and off-the-shelf design. Use of an active building block is emphasized to achieve desired performances for both forms. The electronically tunable active building blocks gained much attention since their synthesized circuits offer good performances for fine-tuning more than tuning the resistance, capacitance or inductance values [6], [7], [8], [9] and [10]. A lately proposed electronically adjustable active analog function block, namely the Voltage Differencing Current Conveyor (VDCC) [11], can be found as a versatile active element for using in many modern circuits [14], [15], [16], [17], [18], [19], [20], [21], [22], [23], [24], [25], [26], [27], [28], [29], [30], [31], [32], [33] and [34]. The most outstanding feature of the circuits using the VDCC is that it gains electronic adjustability.

The VDCC is used in the analog circuit design in both voltage and current-mode for several well-known applications for instance, first-order filter [12], ladder filters [13], passive component simulators/multipliers [11], [14], [15], [16], [17], [18], [19] and [20], square/triangular signal oscillator [21], or sinusoidal signal oscillators [22], [23], [24] and [25]. Several universal or multifunction filters employing VDCCs were introduced [26], [27], [28], [29], [30], [31], [32] and [33]. From our investigation, the filters in [26] and [27] are three-input single-output voltage-mode filter. Also, in [26] the single-input dual-output voltage mode filter is realized.

The filter proposed in [26] and the filter proposed in [27] provide 5 standard function responses comprises only of 1 VDCC cooperating with 1 resistor and 2 capacitors. The filter in [26] consists of 1 VDCC, 2 resistors and 2 capacitors and offers 3 standard functions (LP, HP and BP). The outstanding feature is that the natural frequency and the quality factor can be electronically adjusted. In addition, the adjustment of the quality factor of the second filter in [26] can be achieved without disturbing the natural frequency. Unfortunately, the output voltage terminal is not in low impedance, thus for practical implementation, a voltage buffer is inevitably needed for cascade configuration.

Subsequently, a 1 input 4 output voltage-mode filter proposed in [28] consisting of 1 VDCC, 2 resistors and 2 capacitors, its natural frequency and the quality factor of are tuned with electronic method, where the quality factor is adjusted without disturbing the natural frequency. This voltage-mode filter, however, does not provide low impedance architecture. Later, the current-mode filter using 1 VDCC, 1 dual-output current amplifier, 1 resistor and 2 grounded capacitors was presented in [29]. Its natural frequency is also electronically controlled as well as the quality factor. Moreover, the input and output impedances are ultimately perfect for current-mode architecture without requirement of a current buffer. Unfortunately, the mentioned filter offers only LP, HP, and BR function responses. Additionally, the circuit configuration needs the multiple-output building blocks, which requires more transistors in internal architecture, leading to higher power consumption and more circuit complexity.

The 3 input 1 output current-mode filters composed of 1 VDCC, 1 grounded resistor and 2 grounded capacitors were introduced in [30] and [31]. They offer 5 filter responses while the natural frequency and quality factor are electronically adjustable. As well, the output impedance in current node is high, appropriating for current-mode cascade connection, without any current buffer requirement. The filter introduced in [30], however, requires the multiple-output VDCC. Also, the VDCC based current-mod filter in [31] requires the matching condition for the lowpass filter response.

The single input two output current-mode filters consist of 2 VDCCs, 2 grounded resistors and 2 grounded capacitors were introduced in [32] and [33]. Two output filtering responses are simultaneously obtained while other filtering responses are obtained by summing the input and output currents together. The natural frequency and quality factor are orthogonal adjustable. Moreover, the output impedance in current node is high, appropriating for current-mode cascade connection without any current buffer requirement. However, these require the multiple-output VDCC. Also, these VDCC based current-mode filters require the matching condition for the HP response in [32] and for HP, BR and AP responses in [33]. The comparison of the previous biquad filters and proposed filter using VDCC as active element is shown in Tab. 1.

In this article, a 3 input 1 output transconductance-mode multifunction filter emphasizing on use of VDCCs is proposed. The circuit configuration comprises 3 VDCCs, 3 grounded resistors and 2 grounded capacitors. The features of the proposed filter are that it can be further chip fabrication including off-the-shelf configuration. Additionally, the natural frequency is independently controlled from the quality factor by electronic method. The PSpice simulation and experimental results achieved from the pro-

posed transconductance-mode filter are in corresponding with the theoretical expectation.

The article is organized as follows; Sec. 2. describes principle of operation, the basic principle of the used active elements, VDCC is introduced. The presented transconductance-mode multifunction biquad filter is subsequently explained. Non-ideal analysis of the proposed filter affected from the voltage and current transfer errors is introduced in Sec. 3. Section 4. introduces the simulation and experimental results to prove the different performances of the presented biquad filter. Section 5. provides the conclusion.

2. Principle of the Proposed Circuit

2.1. Active Building Block Used in This Design

The design of transconductance-mode multifunction filter emphasizing on the use of VDCC as the active function block is realized in the paper. So, a brief description of this active element is disclosed in this section.

The internal structure of VDCC for CMOS implementation was initially introduced 2014 by Firat et al [11]. The VDCC is a five-terminals active element. The input and output terminals represent as P, N, Z, X and W terminals. The input voltage terminals, P and N offer the high impedance, where the output current terminals, Z and W achieve high impedance. The voltage output terminal, X is a low impedance. For the conventional VDCC, there are two W terminals called W_n and W_p which provide the output currents in opposite directions. For our design, the VDCC containing only single W terminal is required to achieve practical circuit implementation via commercially available integrated circuits. In addition, avoidance of multiple output terminals can reduce the effect of the current tracking error at W terminal and can additionally decrease the number of transistors inside of VDCC structure. Fig. 1 shows the VDCC circuit symbol including its electrical equivalent circuit. The VDCC ideal electrical characteristics are explained in Eq. (1).

$$\begin{pmatrix} I_N \\ I_P \\ I_Z \\ V_X \\ I_W \end{pmatrix} = \begin{pmatrix} 0 & 0 & 0 & 0 \\ 0 & 0 & 0 & 0 \\ g_m & -g_m & 0 & 0 \\ 0 & 0 & 1 & 0 \\ 0 & 0 & 0 & 1 \end{pmatrix} \begin{pmatrix} V_P \\ V_N \\ V_Z \\ I_X \end{pmatrix}, \quad (1)$$

where g_m represents the transconductance of VDCC. The internal construction of VDCC in this design is implemented using the commercially available Integrated Circuits (ICs) as depicted in Fig. 2(a). It comprises LM13700 as an OTA [34] and AD844 as a current conveyor [35]. This implementation comprises only one terminal without the requirement of W_p or W_n terminal which it can alleviate current tracking error from the current mirrors used in output ports. The g_m for this implementation is obtained as:

$$g_m = \frac{I_B}{2V_T}, \quad (2)$$

where I_B is bias current, V_T is the thermal voltage of approximately 26 mV at a room temperature. It can be seen from Eq. (2) that the g_m is electronically controllable. In Fig. 2(b), the bias current I_B can be simply generated from Microcontroller Unit (MCU). As shown in Fig. 2(b), V_B is the voltage dropped at bias terminal of OTA (for LM13700, V_B is negative) and V_C is controlled voltage sourced from MCU. It is found that the bias current I_B is function of V_C, which is programmable. With this feature, the parameters of the analog circuits using VDCC can be programmable.

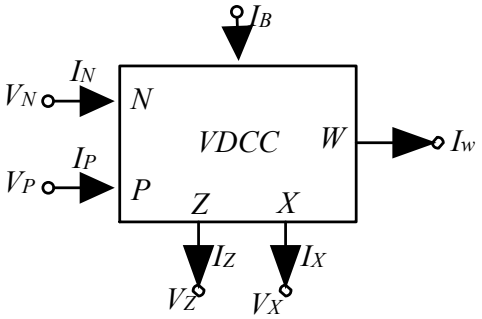

(a) Its electrical symbol.

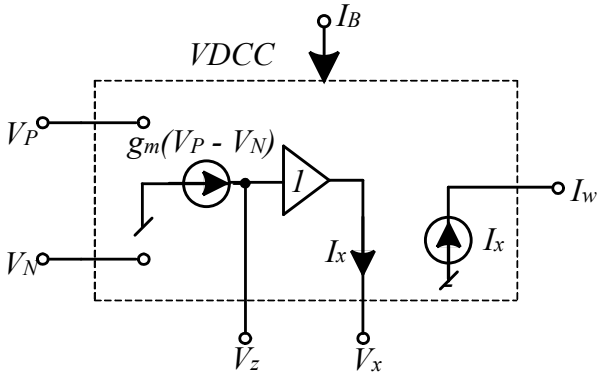

(b) Its equivalent circuit.

Fig. 1: Voltage differencing current conveyor.

Tab. 1: Comparison between various multifunction biquad filers using VDCC as active element.

Ref.	Mode	Filtering category	No. of VDCC	Technology	No. of R+C	All grounded passive element only	Tune of ω_0 and Q	Controllable gain	Cascadability ***	Filtering functions	Results
[26]	VM	MISO (Fig. 2)	1	0.18 µm CMOS & ICs	1+2	No	Non-independent	No	No	LP, HP, BP, BR, AP	Simulation & Experiment
	VM	SIMO (Fig. 3(a))	1	0.18 µm CMOS	2+2	No	Orthogonal	No	No	HP, BP	Simulation
	VM	SIMO (Fig. 3(b))	1	0.18 µm CMOS	2+2	No	Orthogonal	No	No	LP, BP	Simulation
[27]	VM	MISO	1	0.18 µm CMOS	1+2	No	Non-independent	No	No	LP, HP, BP, BR, AP	Simulation
[28]	VM	SIMO	1	HFA3127 & HFA3128 BJT	2+2	No	Orthogonal	No	No	LP, HP, BP, BR	Simulation
[29]	CM	SISO	1*	ICs	1+2	Yes	Non-independent	No	Yes	LP, HP, BR	Simulation & Experiment
[30]	CM	MISO	1	0.18 µm CMOS	1+2	Yes	Non-independent	No	No	LP, HP, BP, BR, AP	Simulation
[31]	CM	MISO	1	0.18 µm CMOS & ICs	1+2	No	Non-independent	No	No	LP, HP, BP, BR, AP	Simulation & Experiment
[32]	CM	SIMO	2	0.18 µm CMOS	2+2	Yes	Orthogonal	No	Yes	LP, BP**	Simulation
[33]	CM	SIMO	2	0.18 µm CMOS	2+2	Yes	Orthogonal	No	Yes	LP, BP**	Simulation & Experiment
Proposed circuit	TM	MISO	3	ICs	3+2	Yes	Independent	Yes	Yes	LP, HP, BP, BR, AP	Simulation & Experiment

* Requires additional Dual Output Current Amplifier (DO-CA).
** In [30] and [33], two output filtering responses (LP and HP) are simultaneously obtained while other filtering responses are obtained by summing the input and output currents together.
*** The cascade-ability is achieved without using additional buffers at both input and output nodes.

2.2. Proposed Transconductance-Mode Multifunction Filter with Electronic Controllability

The proposed electronically controllable transconductance-mode multifunction second order filter is depicted in Fig. 3. It is composed of three VDCCs, three resistors and two capacitors which are connected to ground. It is clear from the circuit in Fig. 3 that the realization of presented filter does not need the VDCC with containing multiple W terminals (W_n or W_p), which is different to the VDCC based current-mode filter proposed in [29] and [30]. From the mentioned principle, the employed VDCC in this design is more suitable to be implemented by employing the commercially available ICs as depicted in Fig. 2. The high input voltage nodes, V_1, V_2 and V_3 are at terminal p of VDCC$_1$, VDCC$_2$ and VDCC$_3$, respectively. The single output current is Io exhibiting a high impedance at the current output terminal. With reference to Fig. 3 and assuming ideal VDCC as shown in Eq. (1), the output current: I_o corresponding to V_1, V_2, and V_3 are is obtained by:

$$I_o = \frac{1}{R_3} \cdot \left(\frac{s^2 V_3 + \frac{g_{m1}}{C_1 R_1 g_{m3}} s V_1 + \frac{g_{m2}}{C_1 C_2 R_1 R_2 g_{m3}} V_2}{s^2 + \frac{g_{m1}}{C_1 R_1 g_{m3}} s + \frac{g_{m2}}{C_1 C_2 R_1 R_2 g_{m3}}} \right). \quad (3)$$

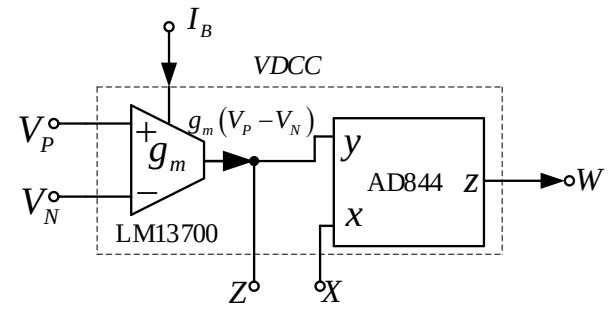

(a) Internal construction.

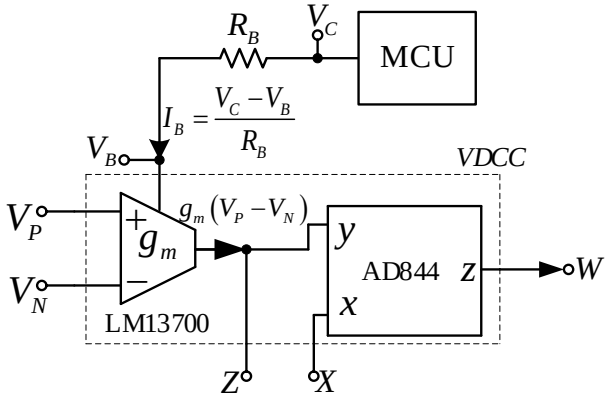

(b) Bias current implementation.

Fig. 2: Practical implementation of VDCC and its bias current.

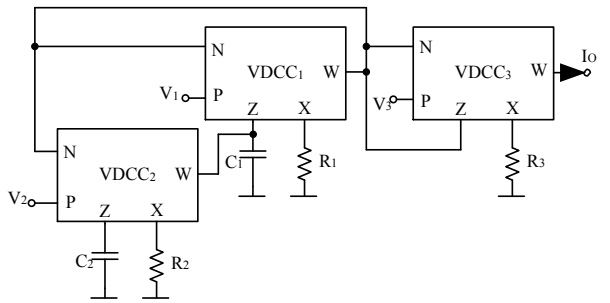

Fig. 3: Proposed multifunction filter.

From Eq. (3), the natural frequency (ω_0) of the presented three input voltage and single input voltage filter is obtained as:

$$\omega_0 = \sqrt{\frac{g_{m2}}{C_1 C_2 R_1 R_2 g_{m3}}}. \tag{4}$$

Also, the quality factor (Q) is provided to be:

$$Q = \frac{1}{g_{m1}} \sqrt{\frac{C_1 R_1 g_{m2} g_{m3}}{C_1 C_2}}. \tag{5}$$

From Eq. (4) and Eq. (5), if $R_1 = R_2 = R$ and $g_{m2} = g_{m3} = g_m$, the natural frequency modified to be:

$$\omega_0 = \frac{1}{R} \sqrt{\frac{1}{C_1 C_2}}. \tag{6}$$

The quality factor in Eq. (5) becomes:

$$Q = \frac{g_m}{g_{m1}} \sqrt{\frac{C_1}{C_2}}. \tag{7}$$

Equation 6 and Eq. (7) verify that the control of the f_0 can be independently set from the Q via resistor R and transconductance g_m, respectively. Additionally, the natural frequency is not temperature sensitive. Also, if g_m and g_{m1} are simultaneously tuned, the quality factor is not temperature sensitive. The transconductance gain for all filtering functions is given by:

$$T(s) = \frac{I_o}{V_{in}} = \frac{1}{R_3}. \tag{8}$$

Derivation of 5 filter functions can be achieved from Eq. (3) as follows:

- By feeding the input signal voltage to node V_2 and connecting nodes V_1 and V_3 to ground, the non-inverting transconductance-mode transfer function for the LP filter is obtained.
- By feeding the input signal voltage to node V_3 and connecting nodes V_1 and V_2 to ground, the non-inverting transconductance-mode transfer function for the HP filter is obtained.
- By feeding the input signal voltage to node V_1 and connecting nodes V_2 and V_3 to ground, the non-inverting transconductance-mode transfer function for the BP filter is obtained.
- By feeding the input signal voltage to node V_2 and connecting nodes V_1 and V_3 to ground, the non-inverting transconductance-mode transfer function for the BR filter is obtained.
- By feeding the input signal voltage to nodes V_2, V_3 and feeding the inverting signal voltage to node V_1, the non-inverting transconductance-mode transfer function for the AP filter is obtained. Thus, the inverting unity voltage amplifier is needed for AP filter.

3. Non-Ideal Consideration

The non-ideal effect of the active element, VDCC on the functionalities of the presented transconductance-mode multifunction biquad filter is considered. Eq. (9) shows the non-idealities of VDCC.

$$\begin{pmatrix} I_N \\ I_P \\ I_Z \\ V_X \\ I_W \end{pmatrix} = \begin{pmatrix} 0 & 0 & 0 & 0 \\ 0 & 0 & 0 & 0 \\ g_m & -g_m & 0 & 0 \\ 0 & 0 & \beta & 0 \\ 0 & 0 & 0 & \alpha \end{pmatrix} \begin{pmatrix} V_P \\ V_N \\ V_Z \\ I_X \end{pmatrix}, \tag{9}$$

where β represents a voltage gain error from the input voltage terminal, Z to the output voltage terminal, X and α represents a current gain error from the input current terminal, X to the output current terminal, W. Taking the non-idealities of VDCC into account and routine analysis, the non-ideal output current of the presented multifunction biquad filter is re-written as:

$$I_o = \frac{\alpha_1\beta_1}{R_3} \cdot \left(\frac{s^2 V_3 + \frac{\alpha_1\beta_1 g_{m1}}{C_1 R_1 g_{m3}} s V_1 + \frac{\alpha_1\beta_1\alpha_2\beta_2 g_{m2}}{C_1 C_2 R_1 R_2 g_{m3}} V_2}{s^2 + \frac{\alpha_1\beta_1 g_{m1}}{C_1 R_1 g_{m3}} s + \frac{\alpha_1\beta_1\alpha_2\beta_2 g_{m2}}{C_1 C_2 R_1 R_2 g_{m3}}} \right). \quad (10)$$

From Eq. (3), the natural frequency non-ideal case is given as:

$$\omega_0 = \sqrt{\frac{\alpha_1\beta_1\alpha_2\beta_2 g_{m2}}{C_1 C_2 R_1 R_2 g_{m3}}}, \quad (11)$$

while, the quality factor for non-ideal case is defined as:

$$Q = \frac{1}{g_{m1}} \sqrt{\frac{\alpha_2\beta_2 g_{m2} g_{m3}}{\alpha_1\beta_1 C_2 R_2}}. \quad (12)$$

It can be noticed from Eq. (11) and Eq. (12), that the voltage/current gain errors in the VDCC directly affect the magnitudes of natural frequency as well as quality factor. Thus, the practically accuracy design of the VDCC must be strictly considered to alleviate the mentioned non-ideal phenomenon. For example, in transistor level design, the high-performance current mirrors are suited to use in the active building blocks.

4. Simulation and Experimental Results

To evaluate and prove several functionalities of the presented transconductance-mode versatile filter with electronic controllability, we provide both program simulation and experimental procedures in this section.

Primarily, the simulation via PSpice was achieved by using the macro model parameters (level 3) of two commercial integrated circuits LM13700 (OTA) and AD844 (CCII) to investigate the workability of the designed transconductance-mode multifunction filter employing the practical realization of the VDCCs as shown in Fig. 2(a). The simulation setting was done as follows; DC bias currents for g_{m1}, g_{m2} and g_{m3} were set to $I_{B1} = I_{B2} = I_{B3} = 100$ µA, while the values of the passive device in the proposed versatile filter were chosen as $R_1 = R_2 = 1.51$ kΩ and $C_1 = C_2 = 1$ nF, the presented transconductance-mode filter was biased by a symmetrical ±5 VDC. Based on device values selected above, the theoretical f_0 calculated from Eq. 4 and the theoretical Q calculated from Eq. 5 are gained respectively to $f_0 = 105.45$ kHz, $Q = 1$ and the transconductance gain is 0.662 mS.

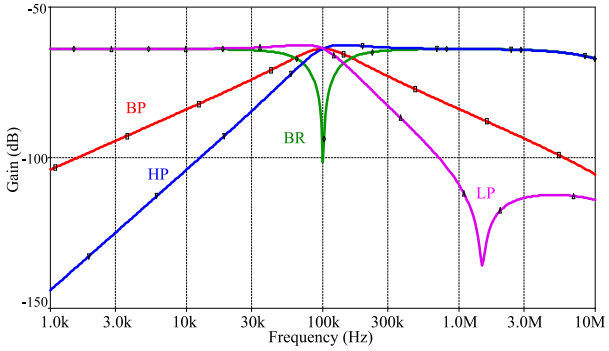

Fig. 4: Gain response of the topology in Fig. 3.

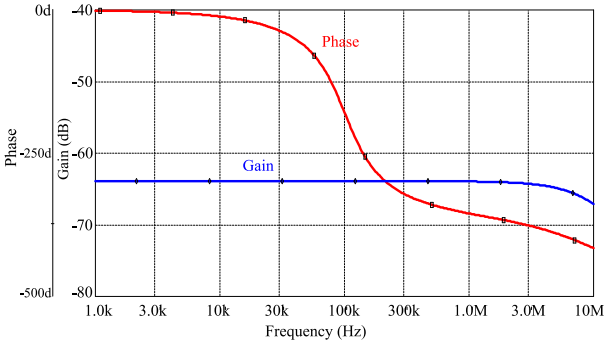

Fig. 5: Simulated phase and gain response of all-pass function.

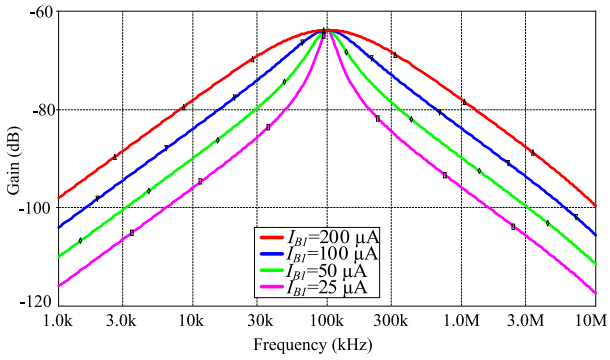

Fig. 6: BP response for different values of I_{B1}.

The simulation result of frequency response for LP, HP, BP, and BR filtering functions achieved from the presented scheme is shown Fig. 4. The simulated f_0 from this simulation is approximately 100 kHz. The deviation of simulated and theoretical value of the natural frequency is about 5.45 %. This deviation stems from the non-ideal effect of VDCC (voltage and current gain errors) as shown in Eq. (10), Eq. (11) and Eq. (12).

The simulation result of AP filtering response which functions as phase shifter is illustrated in Fig. 5. It is found from this result that the simulated gain response is almost constant for whole frequency range, while the phase variation of the output current is changed from 0 ° to −360 °. All mentioned simulation results confirm that the presented transconductance-mode second order filter provides five filtering functions for the same configuration.

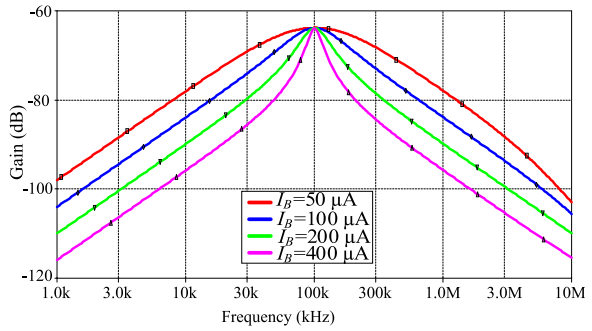

Fig. 7: BP response for different values of I_B ($I_{B2} = I_{B3} = IB$).

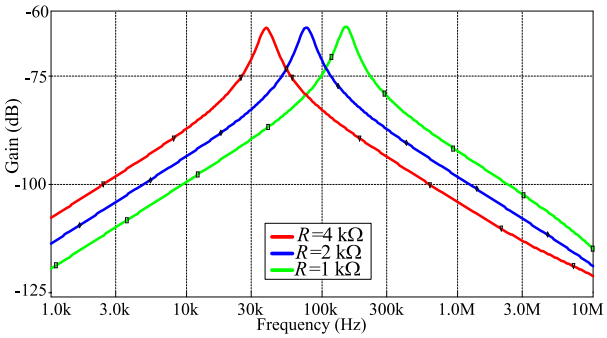

Fig. 8: BP response for different values of R.

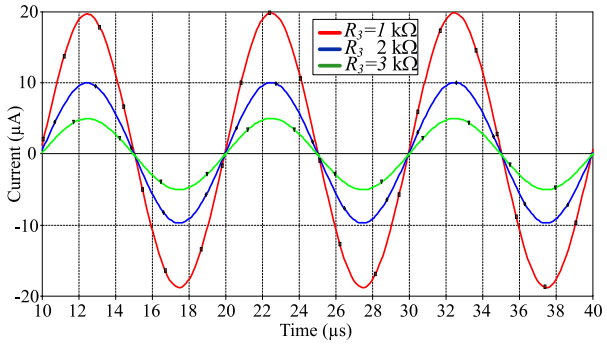

Fig. 9: Output currents for different values of R_3.

The control of Q value without changing the f_0 was proved by the simulation result of frequency response depicted in Fig. 6. In this simulation, the bias current I_{B1} was set for four values, 25 µA, 50 µA, 100 µA and 200 µA. Additionally, the tuning of the Q value can be also controlled without changing the f_0 by simultaneously setting the bias currents $I_{B2} = I_{B3} = I_B$ as the simulation shown in Fig. 7. In this result, $I_{B2} = I_{B3} = I_B$ was adjusted for four values as 50 µA, 100 µA, 200 µA, and 400 µA.

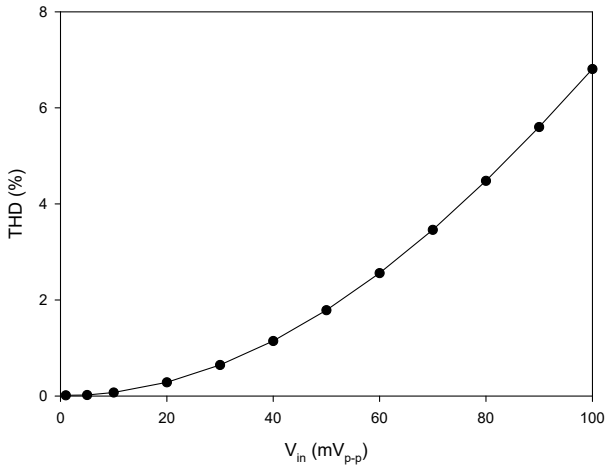

Fig. 10: THD respective to applied sinusoidal input voltage.

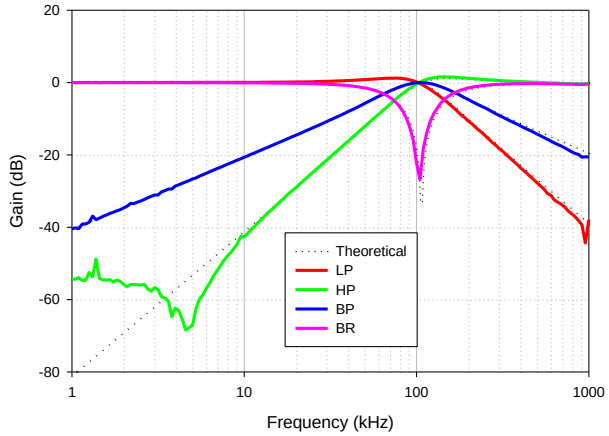

Fig. 11: Experimental gain response of the topology in Fig. 3.

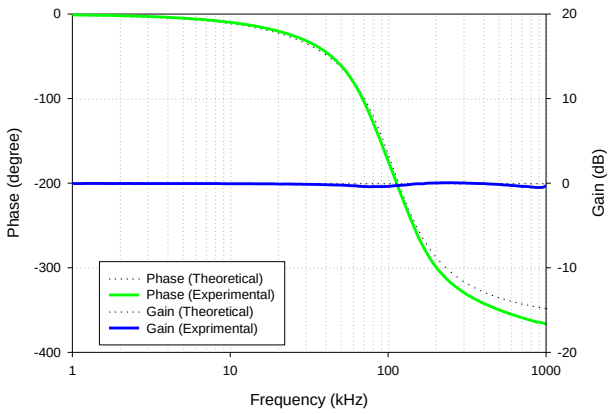

Fig. 12: Experimental phase and gain response of all-pass function.

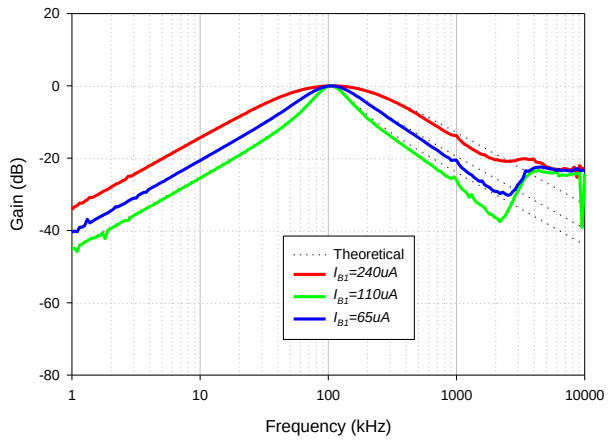

Fig. 13: Experimental BP response for different values of I_{B1}.

The tuning of the f_0 without affecting the Q was proved as depicted in Fig. 8, where $I_{B1} = 25$ µA, $I_{B2} = I_{B3} = 100$ µA, the resistors $R_1 = R_2 = R$ were set for three values as, 1 kΩ, 2 kΩ, and 4 kΩ, the simulated natural frequencies are positioned at 147.91 kHz, 78.85 kHz and 38.91 kHz, respectively. The errors of the simulated and expected f_0 are 7.11 %, 0.96 % and 2.26 %, respectively.

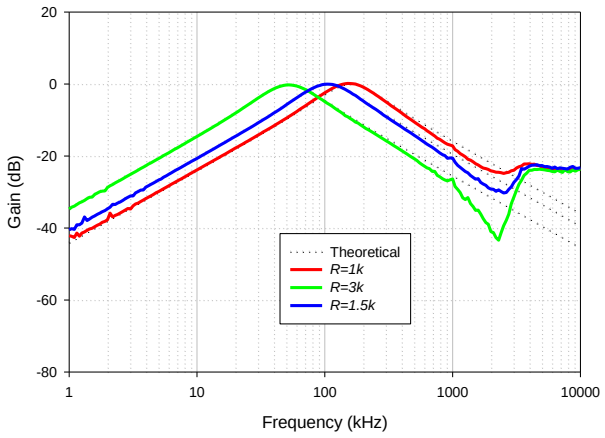

Fig. 14: Experimental BP response for different values of R.

The simulated sinusoidal signal output current in time-domain for band-pass filtering function is depicted in Fig. 9 when resistor R_3 was set for three values as, 1 kΩ, 2 kΩ, and 4 kΩ, the sinusoidal input voltage with 40 $mV_{p\text{-}p}$, $f = 100$ kHz was fed at input voltage node. This simulation result confirms that the output current amplitude of the presented transconductance-mode filter is controlled via R_3. Total Harmonic Distortion (THD) investigation of the proposed transconductance-mode multifunction filter obtained in Fig. 10 was simulated ($f = 100$ kHz).

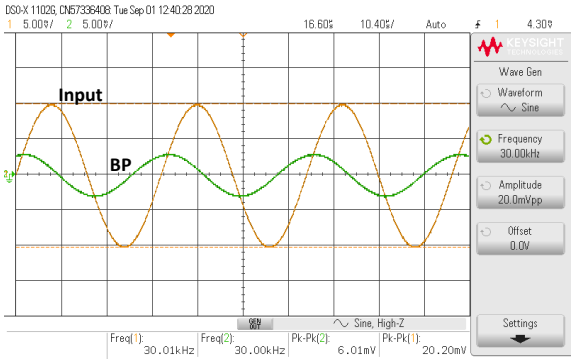

(a) 30 kHz.

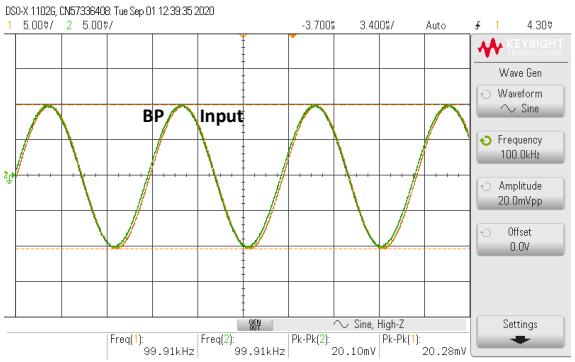

(b) 100 kHz.

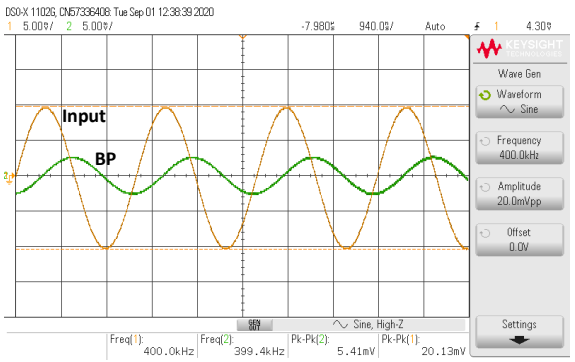

(c) 400 kHz.

Fig. 15: Measurement of input and output waveforms for BP response.

To investigate the practical workability of the proposed transconductance-mode filter, the experiment was also setup by using LM13700 and AD844. The used power supply voltage was ±5 V. The hardware setup was achieved by choosing $C_1 = C_2 = 1$ nF, all resistors were set to be 1.5 kΩ, and all bias currents were 110 µA. The 1.5 kΩ Resistance Load (RL) was connected to the output current node. So, the filter output responses were measured at voltage dropped at RL. Using mentioned element values, the obtained natural frequency as analyzed in Eq. (4) and the quality factor as analyzed in Eq. (5), this yields $f_0 = 106.1$ kHz and $Q = 1$. The measured frequency responses of the

proposed transconductance-mode filter for the LP, HP, BP, and BR functions are shown in Fig. 11. The experimental natural frequency is approximately 104.7 kHz. The deviation of experimental and expected values of the natural frequency is about 1.32 %. Considering the simulation result in Fig. 4 and the experiment result in Fig. 11 it is found that the experimental HP response is affected from the wiring at low frequency.

phase and gain of AP function are depicted in Fig. 14. From the experimental results in Fig. 13 and Fig. 14, it is found that the designed transconductance-mode filter offers five filtering responses as theoretically expected in Subsec. 2.2. The expected and measured gain responses of the filter are trivially different at low and high frequencies due to the effects of non-ideal properties of VDCC, as analyzed in Sec. 3.

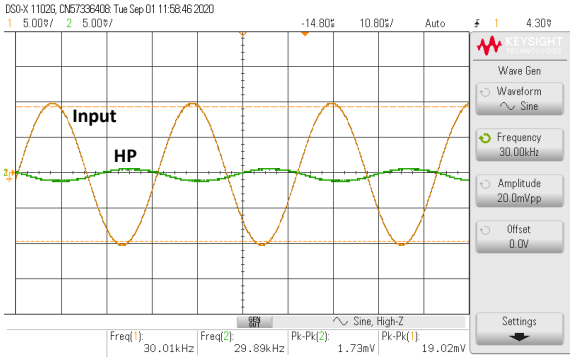

(a) 30 kHz.

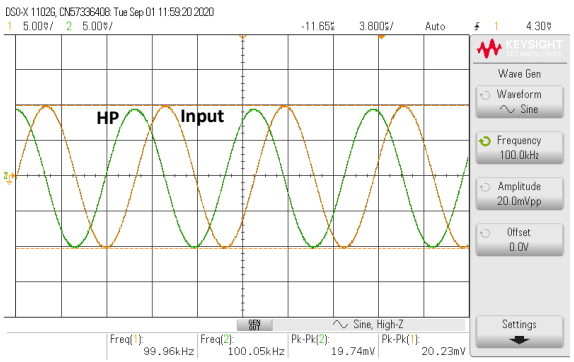

(b) 100 kHz.

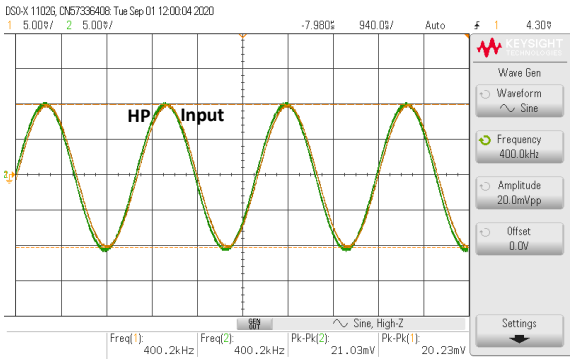

(c) 400 kHz.

Fig. 16: Measurement of input and output waveforms for HP response.

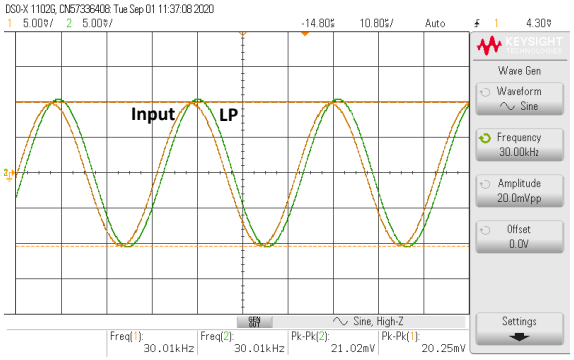

(a) 30 kHz.

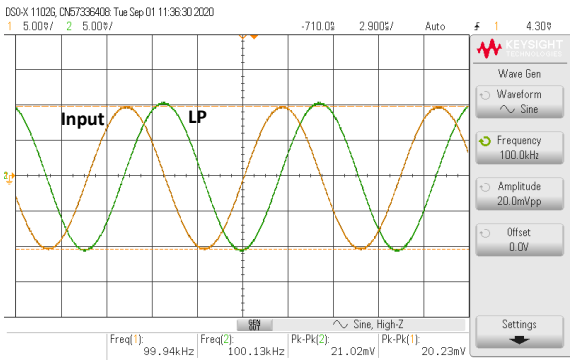

(b) 100 kHz.

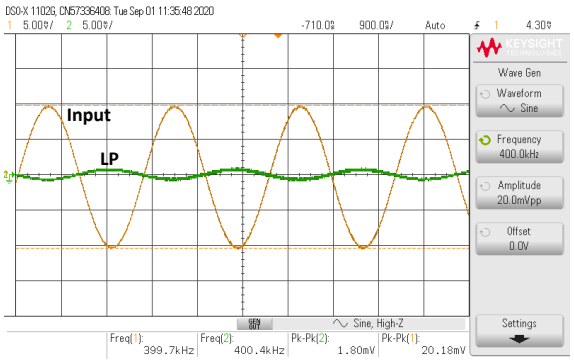

(c) 400 kHz.

Fig. 17: Measurement of input and output waveforms for LP response.

For AP function, the inverting input is required. In experiment, inverting amplifier with unity gain was constructed from a AD844 and two resistors with same resistance value (1.5 kΩ). The frequency response of

The tuning of the Q factor without affecting the f_0 as expected in Eq. (5) was experimentally tested. The experimental result of Q tuning is shown in Fig. 15 where the DC bias current I_{B1} was adjusted for four

values as 65 µA, 110 µA and 240 µA. The tuning of the natural frequency without affecting quality factor as theoretical expected in Eq. (6) was proved as the result shown in Fig. 16, where the resistors $R_1 = R_2 = R$ were set for three values, 1 kΩ, 1.5 kΩ, and 3 kΩ, the natural frequencies obtained from the experiment are located at 151.4 kHz, 104.7 kHz and 52.48 kHz, respectively. The measured input and output transient responses for BP, HP, LP, BR, and AP filter are illustrated in Fig. 15, Fig. 16, Fig. 17, Fig. 18 and Fig. 19, respectively. In mentioned experiment, the 20 mV_{p-p} sinusoidal wave with three values of frequency (30 kHz, 100 kHz and 400 kHz) was applied as input.

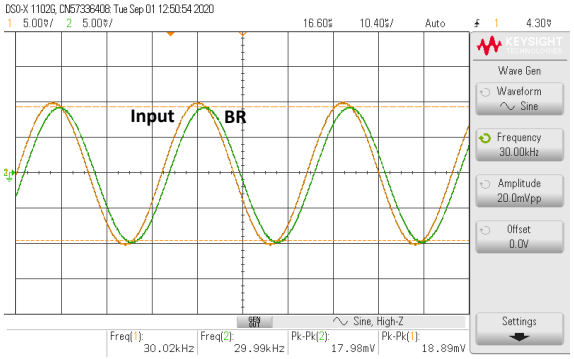

(a) 30 kHz.

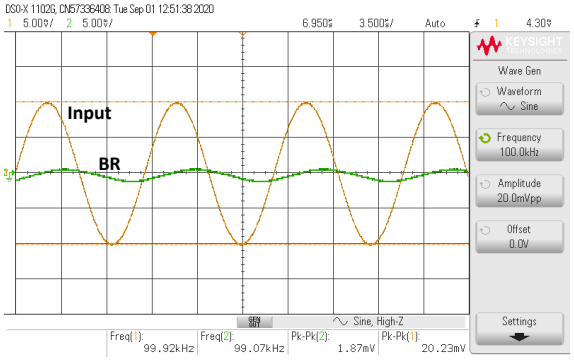

(b) 100 kHz.

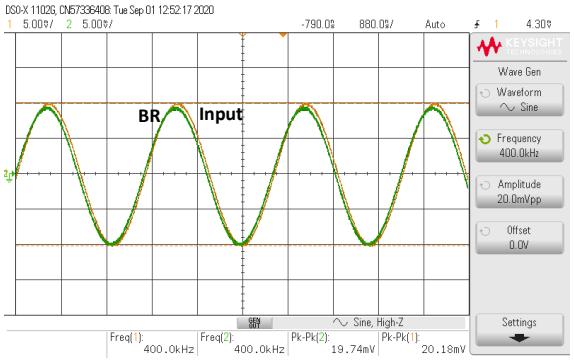

(c) 400 kHz.

Fig. 18: Measurement of input and output waveforms for BR response.

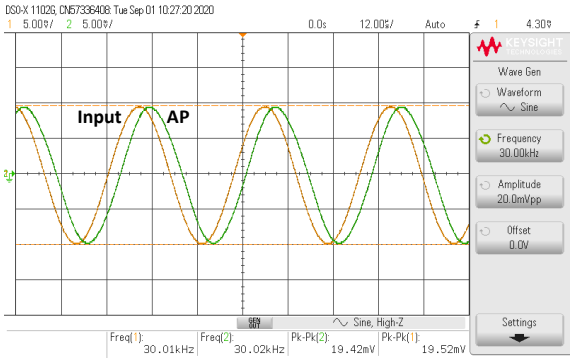

(a) 30 kHz.

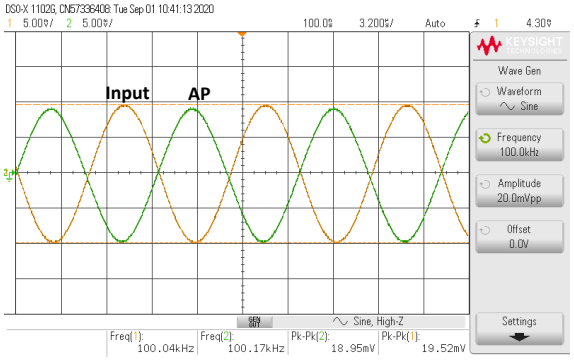

(b) 100 kHz.

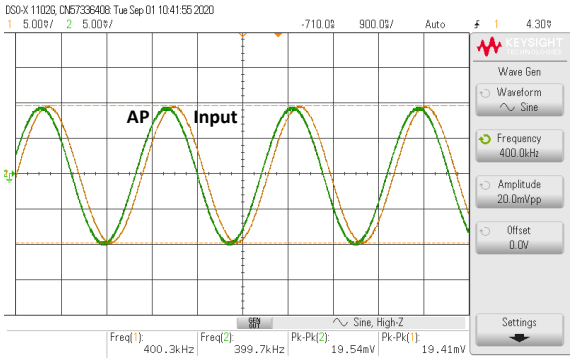

(c) 400 kHz.

Fig. 19: Measurement of input and output waveforms for AP response.

5. Conclusion

The transconductance-mode multifunction second order filter with high input voltage nodes and high output current node has been introduced in this contribution. The proposed filter uses 3 VDCCs without multiple-output to avoid circuit complexity and high power consumption as the active elements cooperating with 3 grounded resistors and 2 grounded capacitors. The standard 5 filter functions can be obtained by suitable input selections. The natural frequency and the quality factor can be adjusted electronically/orthogonally

by controlling the bias currents of the VDCCs, while the output amplitude can be resistively adjusted. Additionally, the natural frequency is not temperature sensitive Also, if g_m and g_{m1} are simultaneously tuned, the quality factor is not temperature sensitive The several performances of the presented versatile filter are demonstrated by both simulation and experimental results, they depict the workability of the presented versatile filter as expected. In addition to using in monolithic chip architecture, based on VDCC implemented from the commercially available ICs, the proposed multifunction filter is also appropriate for off-the-shelf implementation.

Acknowledgment

This work is funded by King Mongkut's University of Technology North Bangkok. Contract no. KMUTNB-GOV-59-16 and Faculty of Industrial Education and Technology, King Mongkut's Institute of Technology Ladkrabang (KMITL).

References

[1] SEDRA, A. S. and K. C. SMITH. *Microelectronic Circuits*. 7th ed. New York: Oxford University Press, 2015. ISBN 978-0199339136.

[2] HERENCSAR, N., O. CICEKOGLU, R. SOTNER, J. KOTON and K. VRBA. New resistorless tunable voltage-mode universal filter using single VDIBA. *Analog Integrated Circuits and Signal Processing*. 2013, vol. 76, iss. 2, pp. 251–260. ISSN 0925-1030. DOI: 10.1007/s10470-013-0090-2.

[3] TOUMAZOU, C., F. J. LIDGEY and D. G. HAIGH. *Analogue IC design: the current-mode approach*. London: The Institution of Electrical Engineers, 2008. ISBN 978-0863412974.

[4] MEKHUM, W., and W. JAIKLA. Resistorless Cascadable Current-Mode Filter Using CCCF-TAS. *Advances in Electrical and Electronic Engineering*. 2013, vol. 11, iss. 6, pp. 501–506. ISSN 1804-3119. DOI: 10.15598/aeee.v11i6.855.

[5] ABDALLA, K. K., D. R. BHASKAR and R. SENANI. Configuration for realising a current mode universal filter and dual-mode quadrature single resistor controlled oscillator. *IET Circuits, Devices & Systems*. 2012, vol. 6, iss. 3, pp. 159–167. ISSN 1751-858X. DOI: 10.1049/iet-cds.2011.0160.

[6] BIOLEK, D., R. SENANI, V. BIOLKOVA and Z. KOLKA. Active Elements for Analog signal processing: Classification, review, and new proposals. *Radioengineering*. 2008, vol. 17, iss. 4, pp. 15–32. ISSN 1805-9600.

[7] KAUR, G., A. Q. ANSARI and M. S. HASHMI. Fractional Order High Pass Filter Based on Operational Transresistance Amplifier with Three Fractional Capacitors of Different Order. *Advances in Electrical and Electronic Engineering*. 2019, vol. 17, iss. 2, pp. 155–166. ISSN 1804-3119. DOI: 10.15598/aeee.v17i2.2998.

[8] BIOLEK, D. and J. VAVRA. Precise Implementation of CDTA. *Advances in Electrical and Electronic Engineering*. 2017, vol. 15, iss. 5, pp. 824–832. ISSN 1804-3119. DOI: 10.15598/aeee.v15i5.2515.

[9] PUSHKAR, K. L. Electronically Controllable Sinusoidal Oscillators Employing VDIBAs. *Advances in Electrical and Electronic Engineering*. 2017, vol. 15, iss. 5, pp. 799–805. ISSN 1804-3119. DOI: 10.15598/aeee.v15i5.2448.

[10] SOTNER, R., J. JERABEK, R. PROKOP and K. VRBA. Current gain controlled CCTA and its application in quadrature oscillator and direct frequency modulator. *Radioengineering*. 2011, vol. 20, iss. 1, pp. 317–326. ISSN 1805-9600.

[11] KACAR, F., A. YESIL, S. MINAEI and H. KUNTMAN. Positive/negative lossy/lossless grounded inductance simulators employing VDCC and only two passive elements. *AEU-International Journal of Electronics and Communications*. 2014, vol. 68, iss. 1, pp. 73–78. ISSN 1434-8411. DOI: 10.1016/j.aeue.2013.08.020.

[12] SOTNER, R., N. HERENCSAR, J. JERABEK, K. VRBA, T. DOSTAL, W. JAIKLA and B. METIN. Novel first-order all-pass filter applications of z-copy voltage differencing current conveyor. *Indian Journal of Pure and Applied Physics*. 2015, vol. 53, iss. 8, pp. 537–545. ISSN 0019-5596.

[13] PRASAD, D., A. AHMAD, A. SHUKLA, A. MUKHOPADHYAY, B. B. SHARMA and M. SRIVASTAVA. Novel VDCC based low-pass and high-pass ladder filters. In: *12th IEEE International Conference Electronics, Energy, Environment, Communication, Computer*. New Delhi: IEEE, 2015 pp. 1–3. ISBN 978-14673-7399-9. DOI: 10.1109/INDICON.2015.7443217.

[14] KARTCI, A., U. E. AYTEN, N. HERENCSAR, R. SOTNER, J. JERABEK and K. VRBA. Application possibilities of VDCC in general floating element simulator circuit. In: *European Conference on Circuit Theory and Design*. Trond-

heim: IEEE, 2015, pp. 1–4. ISBN 978-14799-9877-7. DOI: 10.1109/ECCTD.2015.7300064.

[15] KARTCI, A., U. E. AYTEN, R. SOTNER and R. ARSLANALP. Electronically tunable VDCC-based floating capacitance multiplier. In: *23rd Signal Processing and Communications Applications Conference*. Malatya: IEEE, 2015, pp. 2474–2477. ISBN 978-146737386-9. DOI: 10.1109/SIU.2015.7130385.

[16] KARTCI, A., U. E. AYTEN, N. HERENCSAR, R. SOTNER, J. JERABEK and K. VRBA. Floating capacitance multiplier simulator for grounded RC colpitts oscillator design. In: *International Conference on Applied Electronics*. Pilsen: IEEE, 2015, pp. 93–96. ISBN 978-802610385-1.

[17] PRASAD, D. and J. AHMAD. New Electronically-Controllable Lossless Synthetic Floating Inductance Circuit Using Single VDCC. *Circuits and Systems*. 2014, vol. 5, no. 1, pp. 13–17. ISSN 2153-1293. DOI: 10.4236/cs.2014.51003.

[18] SRIVASTAVA, M. New synthetic grounded FDNR with electronic controllability employing cascaded VDCCs and grounded passive elements. *Journal of Telecommunication, Electronic and Computer Engineering*. 2017, vol. 9, iss. 4, pp. 97–102. ISSN 2180-1843.

[19] GUPTA, P., M. SRIVASTAVA, A. VERMA, A. ALI, A. SINGH and D. AGARWAL. A VDCC-Based Grounded Passive Element Simulator/Scaling Configuration with Electronic Control. *Advances in Signal processing and Communication*. 2019, vol. 526, iss. 1, pp. 429–441. DOI: 10.1007/978-981-13-2553-3_42.

[20] NAVEEN, K., K. PAPPALA, C. MOULI, S. K. Das and M. SRIVASTAVA. Novel Electronic/Resistance Adjustable Capacitance Multiplier Circuit with VDCCs and Grounded Resistances. In: *6th International Conference on Signal Processing and Integrated Networks (SPIN)*. Noida: IEEE, 2019, pp. 1112–1115. ISBN 978-1-7281-1380-7. DOI: 10.1109/SPIN.2019.8711786.

[21] SOTNER, R., J., JERABEK, N. HERENCSAR, T. DOSTAL and K. VRBA. Design of Z-copy controlled-gain voltage differencing current conveyor based adjustable functional generator. *Microelectronics Journal*. 2015, vol. 46, iss. 2, pp. 143–152. ISSN 0026-2692. DOI: 10.1016/j.mejo.2014.11.008.

[22] PRASAD, D., D. R. BHASKAR, and M. SRIVASTAVA. New Single VDCC-based Explicit CurrentMode SRCO Employing All Grounded Passive Components. *Electronics*. 2014, vol. 18, iss. 2, pp. 81–88. ISSN 1450-5843. DOI: 10.7251/ELS1418081P.

[23] SOTNER, R., J. JERABEK, R. PROKOP and V. KLEDROWETZ. Simple CMOS voltage differencing current conveyor-based electronically tunable quadrature oscillator. *Electronics Letters*. 2016, vol. 52, iss. 12, pp. 1016–1018. ISSN 0013-5194. DOI: 10.1049/el.2016.0935.

[24] SRIVASTAVA, M. and D. PRASAD. VDCC Based Dual-Mode Quadrature Sinusoidal Oscillator with Outputs at Appropriate Impedance Levels. *Advances in Electrical and Electronic Engineering*. 2016, vol. 14, iss. 2, pp. 168–177. ISSN 1804-3119 DOI: 10.15598/aeee.v14i2.1611.

[25] SOTNER, R., J. JERABEK, J. PETRZELA and T. DOSTAL. Voltage differencing current conveyor based linearly controllable quadrature oscillators. In: *International Conference on Applied Electronics (AE)*. Pilsen: IEEE, 2016, pp. 237–240. ISBN 978-80-261-0602-9. DOI: 10.1109/AE.2016.7577281.

[26] KACAR, F., A. YESIL and K. GURKAN. Design and experiment of VDCC-based voltage mode universal filter. *Indian Journal of Pure and Applied Physics*. 2015, vol. 53, iss. 5, pp. 341–349. ISSN 0019-5596.

[27] UTTAPHUT, P. Single VDCC-Based Electronically Tunable Voltage-Mode Second Order Universal Filter. *Przeglad Elektrotechniczny*. 2018, vol. 94, iss. 4, pp. 22–25. ISSN 0033-2097. DOI: 10.15199/48.2018.04.06.

[28] SAGBAS, M., U. E. AYTEN, M. KOKSAL and N. HERENCSAR. Electronically tunable universal biquad using a single active component. In: *38th International Conference on Telecommunications and Signal Processing (TSP)*. Prague: IEEE, 2015, pp. 698–702. ISBN 978-147998498-5. DOI: 10.1109/TSP.2015.7296353.

[29] JERABEK, J., R. SOTNER, J. POLAK, K. VRBA and T. DOSTAL. Reconnection-Less Electronically Reconfigurable Filter with Adjustable Gain Using Voltage Differencing Current Conveyor. *Elektronika ir Elektrotechnika*. 2016, vol. 22, no. 6, pp. 39–45. ISSN 1392-1215. DOI: 10.5755/j01.eie.22.6.17221.

[30] LAMUN, P., P. PHATSORNSIRI and U. TORTEANCHAI. Single VDCC-based current-mode universal biquadratic filter. *7th International Conference on Information Technology and Electrical Engineering (ICI-TEE)*. Chiang Mai: IEEE, 2015, pp. 122–125. ISBN 978-146737863-5. DOI: 10.1109/ICI-TEED.2015.7408926.

[31] UTTAPHUT, P. Simple Three-Input Single-Output Current-Mode Universal Filter Using Single VDCC. *International Journal of Electrical and Computer Engineering*. 2018, vol. 8, iss. 6, pp. 4932–4940. ISSN 2088-8708. DOI: 10.11591/ijece.v8i6.pp4932-4940.

[32] GUPTA, M. and T. S. ARORA. Various applications of analog signal processing employing voltage differencing current conveyor and only grounded passive elements: a re-convertible approach. *SN Applied Sciences*. 2020, vol. 2, iss. 9, pp. 1–18. ISSN 2523-3971. DOI: 10.1007/s42452-020-03379-6.

[33] GUPTA, M. and T. S. ARORA. Realization of Current Mode Universal Filter and a Dual-Mode Single Resistance Controlled Quadrature Oscillator Employing VDCC and Only Grounded Passive Elements. *Advances in Electrical and Electronic Engineering*. 2017, vol. 15, iss. 15, pp. 833–845. ISSN 1804-3119. DOI: 10.15598/aeee.v15i5.2397.

[34] LM13700 Dual Operational Transconductance Amplifiers With Linearizing Diodes and Buffers. In: *Texas Instruments* [online]. 2015. Available at: `http://www.ti.com/lit/ds/symlink/lm13700.pdf`.

[35] 60 MHz, 2000 V/µs, Monolithic Op Amp with Quad Low Noise. In: *Analog Devices* [online]. 2017. Available at: `http://www.analog.com/media/en/technical-documentation/data-sheets/AD844.pdf`.

About Authors

Montree SIRIPRUCHYANUN received the B.Tech. Ed. degree in Electrical Engineering from King Mongkut's University of Technology North Bangkok (KMUTNB), the M.Eng. and D.Eng. degree both in electrical engineering from King Mongkut's Institute of Technology Ladkrabang (KMITL), Bangkok, Thailand, in 1994, 2000, and 2004, respectively. He has been with Faculty of Technical Education, KMUTNB since 1994. Presently, he is with Department of Teacher Training in Electrical Engineering as an Associate Professor, KMUTNB. His research interests include analog-digital communications, analog signal processing and analog integrated circuit. He is a member of Institute of Electrical and Electronics Engineers (IEEE), USA, Institute of Electronics, Information and Communication Engineers (IEICE), Japan, and Computer, Communications and Information Technology Association (ECTI), Thailand.

Winai JAIKLA (corresponding author) was born in Buriram, Thailand. He received the B.S.I. Ed. degree in Telecommunication Engineering from King Mongkut's Institute of Technology Ladkrabang (KMITL), Thailand in 2002, M.Tech. Ed. in Electrical Technology and Ph.D. in Electrical Education from King Mongkut's University of Technology North Bangkok (KMUTNB) in 2004 and 2010, respectively. From 2004 to 2011, he was with Electric and Electronic Program, Faculty of Industrial Technology, Suan Sunandha Rajabhat University, Bangkok, Thailand. He has been with the Department of Engineering Education, Faculty of Industrial Education and Technology, King Mongkut's Institute of Technology Ladkrabang, Bangkok, Thailand since 2012. His research interests include electronic communications, analog signal processing, and analog integrated circuits. He is a member of Computer, Communications and Information Technology Association (ECTI), Thailand.